Defective to fully coordinated crossover in complex directionally bonded nanoclusters

Flikkema, Edwin; Bromley, Stefan T.

Published in:
Physical Review B

DOI:
10.1103/PhysRevB.80.035402

Publication date:
2009

Citation for published version (APA):
Flikkema, E., & Bromley, S. T. (2009). Defective to fully coordinated crossover in complex directionally bonded nanoclusters. *Physical Review B*, *80*(3), [035402]. https://doi.org/10.1103/PhysRevB.80.035402

Defective to fully coordinated crossover in complex directionally bonded nanoclusters

E. Flikkema[1] and Stefan T. Bromley[2,3,*]

[1]*Institute of Mathematics and Physics, Penglais, Aberystwyth, Ceredigion SY23 3BZ, United Kingdom*

[2]*Departament de Química Física and Institut de Recerca de Química Teòrica, Universitat de Barcelona, C/Martí i Franquès 1, E-08028 Barcelona, Spain*

[3]*Institució Catalana de Recerca i Estudis Avançats (ICREA), 08010 Barcelona, Spain*

(Received 5 February 2009; revised manuscript received 29 May 2009; published 7 July 2009)

Defect-free fully coordinated (FC) structures are well known to be highly stable for a number of materials exhibiting three-coordinated bonding at the nanoscale (e.g., C_{60}). For topologically more complex nanosystems with higher bonding connectivities the structures and stabilities of the lowest energy FC structures with respect to low-energy defective isomers are unknown. Herein, we describe a general method to thoroughly search through the low-energy geometries of only those nanoclusters that possess FC atomic connectivities. As a pertinent example of our approach we investigate four-connected SiO_2, a fundamentally important network-forming material used in many applications at the nanoscale. Using our method we predict that a structurally complex stability crossover from defective to FC nanoclusters occurs in SiO_2 at a size of ~100 atoms. At variance with previous works, based on constructing FC SiO_2 cagelike nanoclusters by hand, we also show that cagelike clusters are only favored for smaller cluster sizes with dense FC topologies becoming energetically favored with increasing system size.

DOI: 10.1103/PhysRevB.80.035402 PACS number(s): 61.46.Bc, 64.70.Nd, 36.40.Ei

I. INTRODUCTION

Predicting the often complex ways in which terminating ions and atoms of solids rearrange themselves as to lower the total energy is of fundamental scientific and technological importance in understanding materials and how they interact with their chemical, physical, and biological environments. Thus far, experimental and theoretical investigations have primarily concentrated on the structures and properties of the atomically reconstructed regular surfaces of bulk crystalline materials. Of rapidly increasing significance, however, is how the structures of materials with reduced dimensions, often having ill-defined surfaces, adapt to the confines of the nanoscale.

Unlike bulk terminations, for nanoscale materials, it is often difficult to make a clear distinction between surface and interior components. In fact, in many nanosystems the majority of the constituent atoms/ions can be considered to be at or near the terminating boundary of the system and one thus has to consider the possibility of the whole nanostructure undergoing an energy lowering reconstruction. In the ideal case a nanostructure is able to reconstruct into a bonded topology that is fully coordinated (FC) i.e., exhibits no dangling bond defects. Experimentally, carbon and boron nitride are probably the most well known materials to exhibit FC nanoscale structures; often in the form of FC nanocages.[1,2] Theoretical studies of nanoclusters of carbon,[3] XN (for X =B, Al, Ga, and I),[4] ZnO,[5] and ZnS[6] provide strong evidence that the energetic crossover from terminated defective clusters to FC nanocage clusters is quite general in such materials and, moreover, occurs for small cluster sizes ($\leq$26 atoms). For all these materials the nanoscale bonding tends to be coordinated. Formally, within the subspace of small discrete three-connected networks, the number of possible structures is strictly limited and FC cages are among the more likely isomers. For larger sized nanoclusters and on to the bulk polymorphic phases, however, the above-mentioned materials increasingly exhibit four-connected tetrahedral ordering. The extra degree of freedom in networks that allow for four bonds per atomic center allows for a significantly greater number of nanostructure topologies of greater complexity.

In some important materials (e.g., Si and SiO_2) the tendency for four-connectedness does not just steadily emerge with increasing system size but is inherently exhibited in the smallest nanoclusters all the way to the bulk polymorphs. For such structurally complex systems a number of questions remain unresolved concerning the following: (i) the topology of the lowest energy FC nanoclusters, (ii) the existence of a defective-to-FC nanoscale crossover, and (iii) at what system size any crossover may occur. Herein we introduce a general algorithm for finding the low-energy fully reconstructed forms of directionally bonded discrete nanosystems and employ it to investigate the challenging and important case of nanoscale SiO_2. Using our methodology we show that as silica nanoclusters grow in size they increasingly energetically prefer to adopt complex non-cage-like defect-free FC structures that we further predict to become the most stable form of nanosilica beyond a system size of approximately 100 atoms and before the eventual emergence of bulk crystalline structures.

In extended systems, periodic four-connected frameworks may often be physically realized in the bonded atomic structure of crystalline systems of framework-forming tetrahedral materials such as the silica-based zeolites. Although approximately 200 zeolites have thus far been synthesized, ongoing enumerations of periodic tetrahedral frameworks using their representation as abstract graphs have yielded many thousands of hypothetical zeolitic structures.[7] The mathematical enumeration of abstract four-connected graphs having no intrinsic length scale or coordinate system is relatively rapid and formally well defined. The often difficult conversion, however, is from an abstract graph to a realistic three-

dimensional tetrahedrally coordinated material model, if indeed possible at all.[8] Another class of techniques for exploring bulk four-coordinated systems is that of bond transposition (BT) algorithms,[9,10] which are typically applied to amorphous materials (e.g., *a*-SiO_2 and *a*-GaAs). BT algorithms assume that an ideal amorphous solid, although having atoms in noncrystalline positions, should retain the property of being FC; a constraint leading naturally to the continuous random network (CRN) model.[11] As a huge number of CRN representations of a single material always exist, BT algorithms attempt to sample CRNs via a Monte Carlo (MC) sequence of BT moves. In each accepted BT move a chosen pair of bonds (e.g., A-B and C-D) is swapped resulting in two new bonds (e.g., A-C and B-D) and the resulting new bonded configuration and its environment relaxed. BT algorithms operate in real space with periodic boundary conditions and thus provide realistic three-dimensional unit cells without conversion from graph space. Real space periodic systems, however, implicitly constrain the BT moves to be kept local as not to produce disruptive long-range configurational changes for which the relaxation may prove to be impossible. Although a number of BT move types are possible,[12] the inherent locality constraint necessarily limits the arbitrariness of the relaxation process and perhaps, depending on the initial atomic positions, may well significantly slow down, and even forbid, the attainment of very low-energy final states.

II. METHODOLOGY

For discrete nanostructures, unlike in the bulk, there is no periodicity and, in addition to the internal bonding, we must consider also the shape of the nanocluster and the multifarious ways in which it may terminate itself. Due to these complications a thorough unbiased search of the low-energy landscape of fully coordinated nanoclusters of tetrahedral materials is particularly demanding and previous studies have instead concentrated on construction by hand for various systems (e.g., Si,[13] SiO_2,[14–16] and TiO_2[17]).

Taking inspiration from the graph theoretic and BT approaches to periodic systems described above we have developed a MC graph sampling (MCGS) algorithm specifically designed to explore the low-energy landscape of discrete directionally bonded FC nanosystems. The MCGS method starts by considering directionally bonded nanostructures as abstract graphs. Given coordinates for all atoms in a nanostructure the corresponding graph can be defined as follows: (i) nodes correspond to atoms, (ii) for each atom pair an edge is included in the graph if they are bonded; i.e., the distance between the two atoms is below a certain threshold. A FC graph is one where the valency of every node (i.e., the number of edges meeting at that node) is equal to the appropriate chemical valency of the atom represented by that node. In the specific case of $(SiO_2)_N$ clusters the edges in the graph correspond to the Si-O bonds and nodes to Si and O atoms. Further, a graph representation of a FC $(SiO_2)_N$ cluster (i.e., where all valencies are satisfied) is one with alternating nodes of valency two (for O nodes) and four (for Si nodes). As for graph-based zeolite enumeration[8] the most time-consuming part of the MCGS algorithm is finding an optimized three-dimensional cluster geometry corresponding to a particular graph. To avoid excess computation, we thus first screen the topology of each graph. First, we check if a graph has split up into disconnected subgraphs, with any such move rejected. Further, we reject moves to graphs with any two-connected nodes with both connections to a single four-connected node as these correspond to non-FC Si=O terminations. We also reject moves leading to pairs of Si nodes with three common oxygen bridges as this gives unrealistic highly strained geometries (i.e., a triple oxygen bridge) in the corresponding silica nanoclusters. For the remaining graphs we require a corresponding stable atomic configuration in real space to assess the $(SiO_2)_N$ nanocluster energy. After atomically labeling the nodes of the graph we use a series of cost functions consisting of various combinations of the following terms: (i) a bonded harmonic two-body potential for each pair of connected nodes (i.e., {Si-O}) of the form $V_{\text{bond}}=\frac{1}{2}K(r_{ij}-R)^2$, where r_{ij} is the distance between connected nodes and K and R specify the strength and equilibrium distance of the potential respectively, (ii) a harmonic cosine three-body term between each connected triplet of nodes (i.e., {O-Si-O} and {Si-O-Si}), of the form $V_{ABA}=\frac{1}{2}K_{ABA}[\cos(\alpha_{ABA})-\cos(\alpha^0_{ABA})]^2$, where the ABA indices for the angle α_{ABA} and strength parameter K_{ABA} relate to the atom triplets OSiO and SiOSi (with equilibrium angles of 109.47° for α^0_{OSiO} and 180° for α^0_{SiOSi}), and (iii) a nonbonded Buckingham potential together with electrostatics acting between all pairs of nodes (i.e., {Si, O}, {Si,Si}, and {O,O}) that has been parametrized with respect to the geometries and energies of small deformed and optimized $(SiO_2)_N$ clusters.[18]

From randomly generated initial coordinates (corresponding to the real space positions of labeled nodes in a graph) the system energy is first minimized with respect to the harmonic bonded two-body terms and three-body terms. Here the metric-less topology of the graph is converted into a real space object. Here we found it to be imperative that the nonbonded atoms are permitted to freely pass through each other during the optimization significantly reducing the likelihood of becoming trapped in an entangled state. The use of only the connected topology of the graph while ignoring the complications of other interatomic terms is key to quickly finding a reasonable initial nanocluster geometry. The resulting coordinates from this stage are then fed into a second optimization where the three-body terms are switched off while the nonbonded potentials are used to provide repulsion between the atoms to reduce atomic overlaps and to refine the geometry without disrupting the connectivity. Finally, a third stage optimization is performed using only the Buckingham potential and electrostatics. This three-stage cascade of minimizations provides an efficient means to pass from graph space to real space. We note that not every graph will have an energetically stable three-dimensional atomic realization in which case the cascade optimization will lead to a defective geometry. Such defective geometries are detected and eliminated from the list of low-energy FC geometries produced by the algorithm. The MCGS algorithm freely moves through the space of FC graphs (rather than the space of coordinates) using a succession of one or more BT moves. After each graph is changed the decision to accept the up-

dated graph employs a Metropolis Monte Carlo criterion[19] based on the energy change in the optimized atomic cluster geometry from the graph at that step, with respect to that of the previous step. Formally, MC moves between FC graphs are facile, whereas the corresponding actual nanoclusters will often be (i) distant in coordinate space and (ii) separated by high energetic barriers. The MCGS algorithm thus permits a thorough topological exploration of the energy landscape of reconstructed directionally bonded clusters, stepping through this space unhindered by the limitations of the usual locality of BT moves.

III. RESULTS AND DISCUSSION

As a physically relevant demonstration of our method we consider SiO_2: a prototypical network-forming directionally bonded material. Silica is increasingly being employed at the nanoscale as functional nanoparticles, nanofibers, and nanoscale thin films. Defects within and on the surfaces of such nanosilica systems are of great importance with respect to chemical (e.g., reactivity) and physical (e.g., luminescence) properties and their role in performance degradation in some applications (e.g., optics, microelectronics). Very recently, defect-free supported FC nanoscale films of SiO_2 have been experimentally fabricated showing high reactive stability and a unique ability to tailor surface adsorption.[20] From a theoretical perspective FC clusters, due to their finite size yet bulklike atomic connectivity, have been used as models of strained silica systems with respect to their reactivity[21] and vibrational spectra.[22] Similarly, as their defect-free character gives rise to a very stable closed-shell electronic structure, FC nanoclusters have also been used as models for weakly interacting silica coatings of carbon nanotubes[23] and as building blocks for novel discrete cluster-based silica polymorphs.[24,25]

In this study we apply the MCGS method to find the most stable nonterminating FC $(SiO_2)_N$ nanoclusters with increasing size ($N=12,18,24$) and compare them with the proposed correspondingly sized known defective ground states.[26,27] For increased accuracy rather than using energies and structures directly from the MCGS calculations (based on an empirical potential), we refine the results using density-functional theory (DFT). Specifically, for each size, we optimize the 20 lowest energy isomers from the MCGS procedure using the B3LYP hybrid exchange correlation functional[28] and a 6-31G(d,p) basis set with no symmetry constraints, and report the seven lowest energy FC isomers. We note that although DFT generally provides a significant improvement in accuracy with respect classical interatomic potentials in some cases where energetic differences are very small the true energetic ordering should be established from higher level theoretical methods and, when available, experiment.

The results (see Figs. 1–3) show a rich variety of complex FC topologies. For $N=12$ (see Fig. 1) the algorithm was gratifyingly able to find all previously reported FC $(SiO_2)_{12}$ isomers found by manual design and global optimization in a study searching for viable cluster building blocks.[24] In addition our method found a further FC $(SiO_2)_{12}$ cluster (see 1–3 in Fig. 1). We note that the two lowest energy $(SiO_2)_{12}$ FC

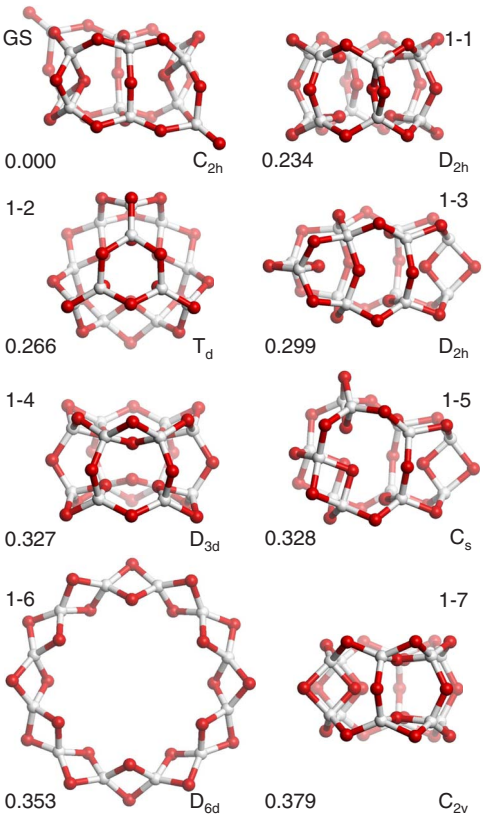

FIG. 1. (Color online) Structures, symmetries, and total energies (eV/SiO_2) of lowest energy $(SiO_2)_{12}$ FC nanoclusters (1–1 to 1–7) relative to the ground state (GS).

isomers (1–1 and 1–2) have all silicon centers with two single Si-O-Si bond connections to two other silicon atoms and one further doubly connected oxygen bridge (a two-ring) to a third silicon center (i.e., these Si atoms have exactly three next-nearest-neighbor Si atoms—denoted Si_T hereafter). In this way we can consider such FC clusters as analogs of atomically three-coordinated polyhedral cages, whereby cluster 1–1 can be viewed as a six-ring prismatic polyhedron and cluster 1–2 as a truncated tetrahedron.[14] In all the following we will describe FC silica clusters with such Si_T-based topologies as cagelike. For $N=18$ (see Fig. 2) the MCGS method finds that all low-energy isomers are cagelike. Moreover, we find a cagelike FC structure (2–1 in Fig. 2) that is 0.27 eV lower in total energy than the lowest energy previously reported $(SiO_2)_{18}$ cagelike construction (see 2–2 in Fig. 2 and Ref. 14). In addition, all other low-energy FC $(SiO_2)_{18}$ isomers are reported and all lower in energy than the only other reported FC $(SiO_2)_{18}$ cagelike isomer we could find,[29] which was manually constructed by joining two and three-membered $(SiO)_n$ rings. The results for $N=24$ are, however, the most striking, with the MCGS procedure finding six more energetically stable isomers (i.e., 3–1 to 3–6 in Fig. 3) than the most stable previously reported $(SiO_2)_{24}$ (cagelike) isomer[14] (see 3–7 in Fig. 3). Of particular note is the fact that as we go from clusters 3–7 to 3–1 the number of silicon centers having a cagelike "triply" connected character tends to decrease: 24 Si_T centers for cluster 3–7, 16 Si_T centers for clusters 3–6 and 3–4, 14 Si_T centers for clusters 3–5,

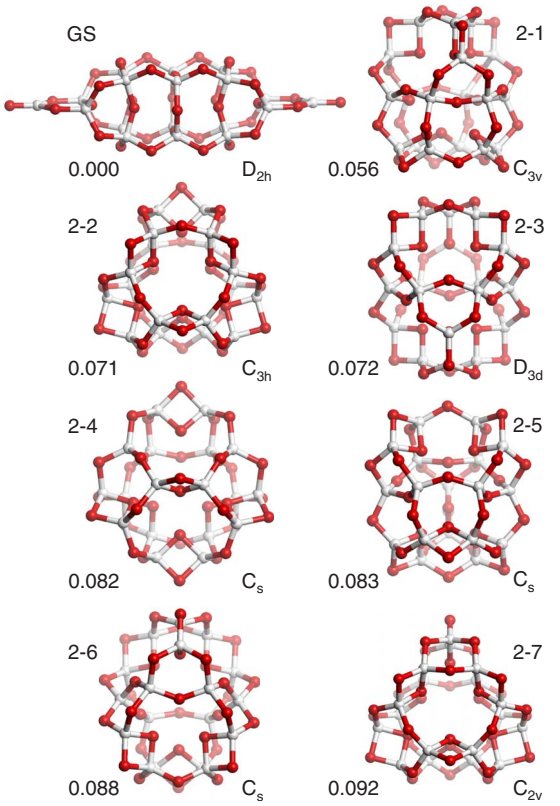

FIG. 2. (Color online) Structures, symmetries, and total energies (eV/SiO_2) of lowest energy $(SiO_2)_{18}$ FC nanoclusters (2–1 to 2–7) relative to the ground state (GS).

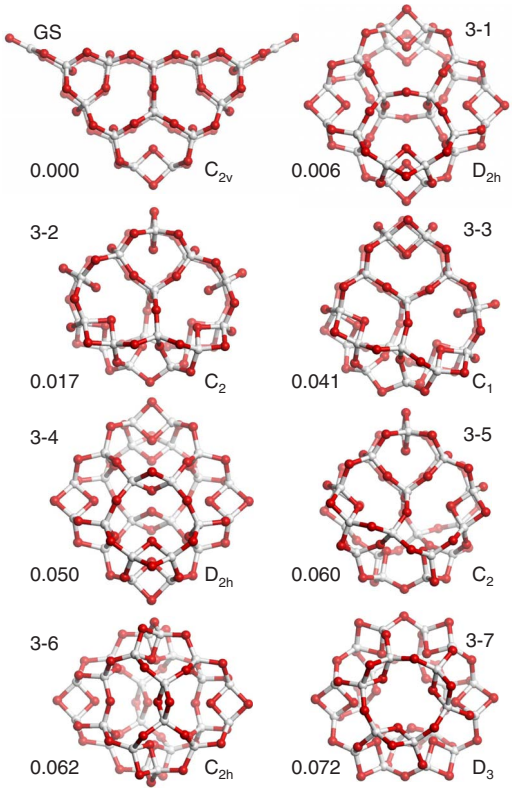

FIG. 3. (Color online) Structures, symmetries, and total energies (eV/SiO_2) of lowest energy $(SiO_2)_{24}$ FC nanoclusters (3–1 to 3–7) relative to the ground state (GS).

3–3, and 3–2, and 12 Si_T centers for cluster 3–1). This topological change is also accompanied by a shift in preferred cluster morphology, whereby the spherical open cagelike form of 3–7 progressively gives way to increasingly stable and increasingly flattened disklike cluster forms. Interestingly, the planar structure of the lowest energy $(SiO_2)_{24}$ disk (3–1) is reminiscent of that found in fully reconstructed SiO_2 supported monolayers[20] and also similar in form to the likely (defective) ground states for $(SiO_2)_N$ $N>24$.[27] Further, we note that when considering all known $(SiO_2)_{24}$ isomers the 3–1 $(SiO_2)_{24}$ flattened disk is only marginally higher in energy than the oxygen-terminated $(SiO_2)_{24}$ global ground state[27] with which it is essentially energetically degenerate (see Fig. 3). This finding strongly suggests that FC silica cages previously calculated for well over 150 atoms[15,16] are not the most stable FC nanoscale topology for systems of 72 atoms and larger.

Plotting the total energy per SiO_2 unit of each of the lowest energy FC isomers and of the correspondingly sized terminated ground state[27] (see Fig. 4) we see that the two lines quickly converge with increasing cluster size. Taking the total energy difference between the two cluster classes and fitting with a power law provides a rough prediction as to the relative stability of each cluster type with further increase in size. This approximate extrapolation indicates that the lowest energy FC clusters will become the energetic global ground states for cluster $(SiO_2)_N$ sizes $N \geq 26$. Unfortunately, limits on the increasing unreliability of available interatomic potentials (with respect to DFT) for this size range,[30] together with the exponentially increasing size of the cluster isomer search space, mean that we currently are unable to reliably test this prediction directly. As a demonstration of the former problem we show in Fig. 5 the relative total energies of three FC clusters (4–1, 4–2, and 4–3) containing 90 atoms (i.e., composition $Si_{30}O_{60}$) as computed by three commonly used interatomic potentials (BKS,[31] TTAM,[32] and FB[18]) with respect to that calculated using DFT. We first note that the FC $Si_{30}O_{60}$ clusters in Fig. 5 are not predicted to be particularly energetically stable isomers (with respect to DFT) but rather are presented as an illustrative case study. For each interatomic potential we can see that the energetic ordering as predicted by DFT is not recovered. For the BKS and TTAM potentials, cluster 4–2 is predicted to be more stable than cluster 4–1 by 0.09–0.1 eV/SiO_2 while cluster 4–3 appears to be particularly unstable for these potentials (0.24–0.28 eV/SiO_2 less stable). Conversely, for the FB potential, which was specifically parametrized for silica nanoclusters,[18] cluster 4–1 is, correctly, slightly lower in energy than cluster 4–2. However, in this case the cluster 4–3 is predicted to be significantly lower in energy than 4–1 (by 0.084 eV/SiO_2), at odds with the DFT computed stability order. This divergence between the predictions of interatomic potentials (essential for rapid evaluation of cluster energies in the MCGS algorithm) and DFT is present at all cluster sizes but can be accommodated for as long as one accurately evaluates (e.g., via energy minimization using DFT) a sufficiently large subset of clusters resulting from the MCGS in order to establish the ground state. Although for smaller clus-

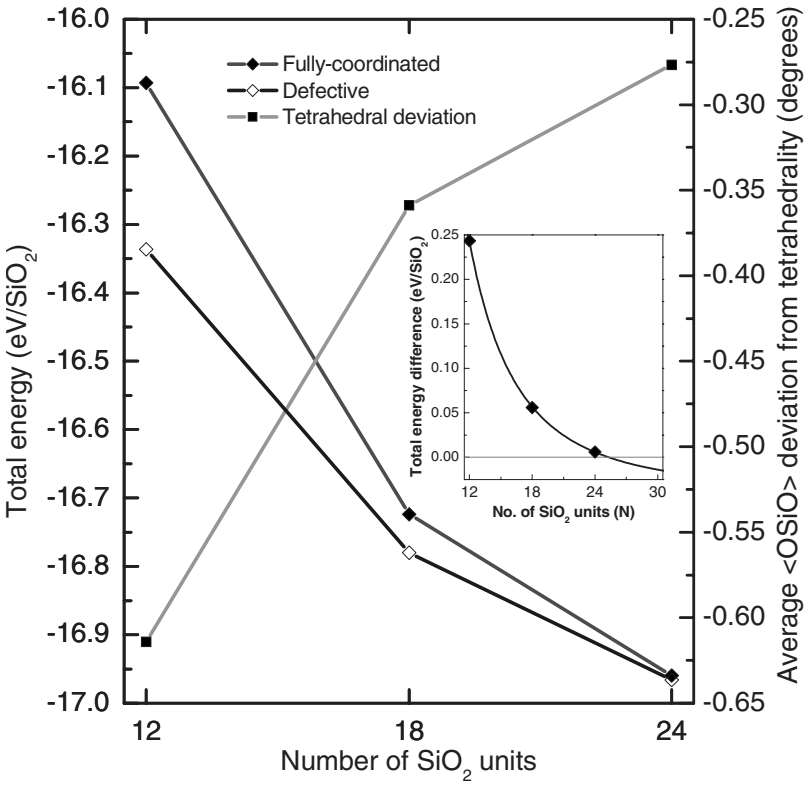

FIG. 4. Total energies and average deviation from tetrahedrality of GS and lowest energy FC $(SiO_2)_N$ nanoclusters for $N=12,18,24$ (inset: power-law fit to the total energy difference between correspondingly sized GS and lowest energy FC clusters).

ter sizes this is practicable, for moderately large clusters this problem appears to be particularly acute. Probable reasons for this problem include the massive increase in the number of isomer possibilities for larger cluster sizes (possibly allowing for more diverse structures and more opportunity for spurious low-energy clusters) and the mismatch between the potential parametrization (bulk or small nanocluster) and the system size being probed.

Based upon our results for $(SiO_2)_N$ clusters for $N=12-24$, which strongly suggest that FC systems eventually dominate the low-energy landscape of nanosilica, it is interesting to enquire what the driving force for this transition could be. For all studied sizes the FC clusters exhibit numerous local surface reconstructions consisting of variable numbers of Si_2O_2 two-rings. For the largest size considered we see that the terminated $(SiO_2)_{24}$ ground state has two silanone (Si=O) terminations and one two-ring whereas the lowest energy FC $(SiO_2)_{24}$ disk isomer has six two-rings. Recent DFT calculations of larger nonglobally optimized compressed nanoslabs of 36 to 48 SiO_2 units have also observed a competition between silanones and two-rings as surface-energy-reducing mechanisms, noting also that their formation is largely determined by the local bonding environment.[33] As the reaction between two separated silanones to make a FC two-ring is an energetically favorable barrierless process,[34] depending on the constraints of the bonding topology of the cluster we would expect all silanone terminations to eventually lose out to FC two-rings. Experimentally it is known that two-rings form on annealed thin amorphous silica films[35] and previously we have demonstrated the size dependency of the transition from two Si=O defects to a two-ring in a model nanochain-to-nanoring system.[36] In this system we also noted a transition in the electronic structure, whereby, when the energy of two-ring formation was lower than that of having silanone terminations, the electronic energy gap in the system also became larger. We note that in the present case the calculated energy gap of the $(SiO_2)_{24}$ disk is 0.23 eV higher than the silanone terminated $(SiO_2)_{24}$ ground state (6.16 eV versus 5.93 eV, respectively) indicating a greater electronic stability for the FC structure. Although the stability of an isolated terminal silanone is expected to be relatively constant, the strain in a closed two-ring is known to be significantly affected by its local bonded environment.[37] This is clearly seen by comparing the FC $(SiO_2)_{24}$ isomers 3–2, 3–3, and 3–5, which all have seven two-rings but different energies. We also note that the lowest energy FC disk (3–1 in Fig. 3) has the lowest number of two-rings in the set of $(SiO_2)_{24}$ FC isomers. This suggests that with increasing size low-energy FC topologies will employ proportionally fewer and fewer strained two-

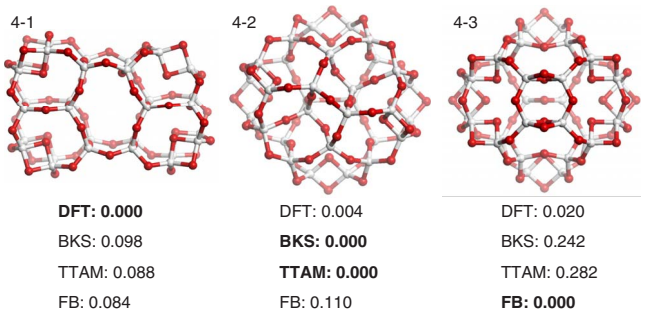

FIG. 5. (Color online) Comparison of total energy differences (eV/SiO_2) between three FC $Si_{30}O_{60}$ (4–1 to 4–3) clusters as calculated by DFT (B3LYP/6-31G*) and the potentials: BKS (Ref. 31), TTAM (Ref. 32), and FB (Ref. 18).

rings to achieve a particular FC topology. Examining the ratio of two-rings to single Si-O-Si bonds in the lowest energy FC isomers with increasing size we indeed observe such a trend [0.6 for $(SiO_2)_{12}$, 0.25 for $(SiO_2)_{18}$, and 0.17 for $(SiO_2)_{24}$]. With increasing size we expect that generally the internal bonded strain will gradually reduce further energetically favoring FC geometries. In Fig. 4 the average O-Si-O angle (a measure of tetrahedral strain) is also plotted (with respect to the optimal unstrained value of 109.47°) for the lowest energy FC clusters showing also the internal bonding strain reduces with increasing cluster size.

IV. CONCLUSIONS

In summary, in low-energy nanosilica systems we show that FC $(SiO_2)_N$ nanoclusters become increasingly energetically competitive with known defective ground states with increasing size and are likely ground-state candidates for $N \geq 26$. The defective-to-FC crossover is found to be topologically complex and quite unlike that for three-connected nanosystems (i.e., not cagelike). We speculate that such size-dependent crossovers are likely to be exhibited in many directionally bonded nanosystems (e.g., GaAs) and, due to the characteristic topologies of FC over defective nanosystems, to be accompanied by significant and potentially useful changes in chemical and physical properties.

ACKNOWLEDGMENTS

E.F. wishes to acknowledge that part of this research was supported by a Marie Curie Intra-European Fellowship (MEIF-CT-2005-011551) within the 6th European Community Framework Program. E.F. is in receipt of an RCUK Academic Fellowship. S.T.B. acknowledges support from the Spanish Ministry for Science and Innovation (Grant No. FIS2008-02238/FIS) and from the COST-D41 action.

*Corresponding author.

[1] H. W. Kroto, J. R. Heath, S. C. O'Brien, R. F. Curl, and R. E. Smalley, Nature (London) **318**, 162 (1985).
[2] D. Golberg, Y. Bando, O. Stéphan, and K. Kurashima, Appl. Phys. Lett. **73**, 2441 (1998).
[3] P. R. C. Kent, M. D. Towler, R. J. Needs, and G. Rajagopal, Phys. Rev. B **62**, 15394 (2000).
[4] S. A. Shevlin, Z. X. Guo, H. J. J. van Dam, P. Sherwood, C. R. A. Catlow, A. A. Sokol, and S. M. Woodley, Phys. Chem. Chem. Phys. **10**, 1944 (2008).
[5] A. A. Al-Sunaidi, A. A. Sokol, C. R. A. Catlow, and S. M. Woodley, J. Phys. Chem. C **112**, 18860 (2008).
[6] E. Spanó, S. Hamad, and C. R. A. Catlow, J. Phys. Chem. B **107**, 10337 (2003).
[7] M. M. Treacy, I. Rivin, E. Bakovsky, K. H. Randall, and M. D. Foster, Microporous Mesoporous Mater. **74**, 121 (2004).
[8] S. A. Wells, M. M. Treacy, and M. D. Foster, Microporous Mesoporous Mater. **93**, 151 (2006).
[9] F. Wooten, K. Winer, and D. Weaire, Phys. Rev. Lett. **54**, 1392 (1985).
[10] N. Mousseau and G. T. Barkema, Curr. Opin. Solid State Mater. Sci. **5**, 497 (2001).
[11] W. H. Zachariasen, J. Am. Chem. Soc. **54**, 3841 (1932).
[12] T. S. Hudson and P. Harrowell, J. Chem. Phys. **126**, 184502 (2007).
[13] E. Kaxiras, Phys. Rev. Lett. **64**, 551 (1990).
[14] S. T. Bromley, Nano Lett. **4**, 1427 (2004).
[15] D. Zhang, J. Wu, R. Q. Zhang, and C. Liu, J. Phys. Chem. B **110**, 17757 (2006).
[16] M. Linnolahti, N. M. Kinnunen, and T. Pakkanen, Chem. Eur. J. **12**, 218 (2006).
[17] Z.-W. Qu and G.-J. Kroes, J. Phys. Chem. C **111**, 16808 (2007).
[18] E. Flikkema and S. T. Bromley, Chem. Phys. Lett. **378**, 622 (2003).
[19] N. Metropolis, A. Rosenbluth, M. Rosenbluth, A. Teller, and E. Teller, J. Chem. Phys. **21**, 1087 (1953).
[20] S. Ulrich, N. Nilius, H.-J. Freund, U. Martinez, L. Giordano, and G. Pacchioni, Phys. Rev. Lett. **102**, 016102 (2009).
[21] N. de Leeuw, Z. Du, J. Li, S. Yip, and T. Zhu, Nano Lett. **3**, 1347 (2003).
[22] S. T. Bromley, M. A. Zwijnenburg, and Th. Maschmeyer, Surf. Sci. **539**, L554 (2003).
[23] J. C. Wojdel and S. T. Bromley, J. Phys. Chem. B **109**, 1387 (2005).
[24] S. T. Bromley and E. Flikkema, Comput. Mater. Sci. **35**, 382 (2006).
[25] S. T. Bromley, Cryst. Eng. Comm. **9**, 463 (2007).
[26] E. Flikkema and S. T. Bromley, J. Phys. Chem. B **108**, 9638 (2004).
[27] S. T. Bromley and E. Flikkema, Phys. Rev. Lett. **95**, 185505 (2005).
[28] P. J. Stephens, F. J. Devlin, C. F. Chabalowski, and M. J. Frisch, J. Phys. Chem. **98**, 11623 (1994).
[29] D. Zhang, M. Zhao, and R. Q. Zhang, J. Phys. Chem. B **108**, 18451 (2004).
[30] S. T. Bromley, Phys. Status Solidi A **203**, 1319 (2006).
[31] B. W. H. van Beest, G. J. Kramer, and R. A. van Santen, Phys. Rev. Lett. **64**, 1955 (1990).
[32] S. Tsuneyuki, M. Tsukada, H. Aoki, and Y. Matsui, Phys. Rev. Lett. **61**, 869 (1988).
[33] C.-L. Kuo, S. Lee, and G. S. Hwang, Phys. Rev. Lett. **100**, 076104 (2008).
[34] P. V. Avramov, I. Adomovic, K. M. Ho, C. Z. Wang, W. C. Lu, and M. S. Gordon, J. Phys. Chem. A **109**, 6294 (2005).
[35] C. M. Chiang, B. R. Zegarski, and L. H. Dubois, J. Phys. Chem. **97**, 6948 (1993).
[36] S. T. Bromley, M. A. Zwijnenburg, and Th. Maschmeyer, Phys. Rev. Lett. **90**, 035502 (2003).
[37] S. T. Bromley, I. P. R. Moreira, F. Illas, and J. C. Wojdel, Phys. Rev. B **73**, 134202 (2006).